

## Unusual high-temperature ferromagnetism of $\text{PbPd}_{0.81}\text{Co}_{0.19}\text{O}_2$ nanograin film

H. L. Su,<sup>1,2,3</sup> S. Y. Huang,<sup>2</sup> Y. F. Chiang,<sup>2,4</sup> J. C. A. Huang,<sup>2,4,a)</sup> C. C. Kuo,<sup>5,b)</sup> Y. W. Du,<sup>3</sup> Y. C. Wu,<sup>1</sup> and R. Z. Zuo<sup>1</sup>

<sup>1</sup>*School of Materials Science and Engineering, Hefei University of Technology, Hefei 230009, People's Republic of China*

<sup>2</sup>*Department of Physics, National Cheng Kung University, Tainan 701, Taiwan*

<sup>3</sup>*National Laboratory of Solid State Microstructure and Department of Physics, Nanjing University, Nanjing 210093, People's Republic of China*

<sup>4</sup>*Advanced Optoelectronic Technology Center and Center for Micro/Nano Science and Technology, National Cheng Kung University, Tainan 701, Taiwan*

<sup>5</sup>*Department of Physics, National Sun-Yat-Sen University, Kaohsiung 804, Taiwan*

(Received 16 April 2011; accepted 14 August 2011; published online 8 September 2011)

Single-phase  $\text{PbPd}_{0.81}\text{Co}_{0.19}\text{O}_2$  film with a body-centered orthorhombic structure was prepared using the sol-gel spin-coating technique and an oxidation treatment. Film resistivity has a power dependence on temperature. The insulator-metal transition temperature was 358 K, markedly higher than the reported values of similar material systems. Ferromagnetism and superparamagnetism coexisted in the film and the ferromagnetism persisted up to 380 K. As temperature increased, the notable increasing tendencies were found for the film's saturation magnetization and for the magnetic field where saturation magnetization decreases abruptly. The special spin gapless band structure and the film's nanograin microstructure are likely responsible for these interesting properties. © 2011 American Institute of Physics. [doi:10.1063/1.3634070]

Inspired by the excellent performance of gapless semiconductors and graphene, a spin gapless semiconductor (SGS) was developed by Wang in 2008.<sup>1</sup> This material has both high spin polarization and long spin relaxation lengths theoretically, making it attractive as a potential spintronic material after the development of the half-metal and the diluted magnetic semiconductor.<sup>1-4</sup> As reported, the spin gapless feature can be generated by introducing foreign ions or vacancies into a gapless or narrow-gap material.<sup>1,5-7</sup> Because  $\text{PbPdO}_2$  is the only oxide gapless semiconductor without toxic elements, such as Hg and Te, it is considered as the most suitable matrix material for studies of SGSs.<sup>1-4,8</sup> The energy band structure and transport and magnetic properties of  $\text{PbPdO}_2$  doped with Co and Mn ions have been studied theoretically and experimentally.<sup>1-4</sup> The low-temperature colossal electroresistance and giant magnetoresistance effects were obtained within  $\text{PbPd}_{0.75}\text{Co}_{0.25}\text{O}_2$ , and the low-temperature ferromagnetisms were found within  $\text{PbPd}_{0.9}\text{Co}_{0.1}\text{O}_2$  and  $\text{PbPd}_{0.9}\text{Mn}_{0.1}\text{O}_2$ .<sup>2-4</sup> In this letter, we report the interesting electric and magnetic properties of  $\text{PbPd}_{0.81}\text{Co}_{0.19}\text{O}_2$  nanograin film.

The  $\text{PbPd}_{0.81}\text{Co}_{0.19}\text{O}_2$  thin film was deposited using the sol-gel spin-coating technique and an oxidation treatment. The sol was prepared as reported previously.<sup>9</sup> The raw materials used were  $\text{Pb}(\text{NO}_3)_2$ ,  $\text{Pd}(\text{NO}_3)_2 \cdot 2\text{H}_2\text{O}$ , and  $\text{Co}(\text{NO}_3)_2 \cdot 6\text{H}_2\text{O}$ , the chelating agent was citric acid monohydrate, and the solvent was ethylene glycol, and an additional 5 mol. %  $\text{Pb}(\text{NO}_3)_2$  was adopted to compensate for the loss of Pb during

the subsequent heat treatment. To obtain precursor films, the sol was spin-coated onto (1 $\bar{1}$ 02) sapphire substrates at 3000 rpm for 30 s. The as-coated precursor films were dried in air at 75 °C and then oxidized at 430 °C in ambient oxygen for 5 min. These coating and oxidizing treatments were repeated 4 times to obtain a film thickness of roughly 110 nm. This was followed by the final calcination at 700 °C for 10 min under an oxygen atmosphere.

The surface image (Fig. 1) and the composition of the formed film were measured using a scanning electron microscope (SEM) equipped with an energy dispersive x-ray analyzer. The film had a nanograin structure with an average grain size of roughly 22 nm. The Pb:Pd:Co atomic ratio was 100:81:19. The film's crystalline structure was characterized by x-ray diffraction (XRD) using  $\text{Cu K}\alpha$  radiation. The inset of Fig. 1 shows the film's XRD pattern. Clearly, the film is single phase with a body-centered orthorhombic structure.

Fig. 2(a) shows the temperature ( $T$ ) dependence of the film's resistivity ( $\rho$ ) measured at a constant current of 1  $\mu\text{A}$  using a physical properties measurement system (PPMS). Both resistivity and its variation ratio for the sample were higher than those of  $\text{PbPd}_{0.9}\text{Co}_{0.1}\text{O}_2$  and  $\text{PbPd}_{0.9}\text{Mn}_{0.1}\text{O}_2$  bulks, but less than those of the  $\text{PbPd}_{0.75}\text{Co}_{0.25}\text{O}_2$  film prepared by pulsed laser deposition.<sup>2-4</sup> Moreover, its  $T_{\text{MI}}$  was roughly 358 K, much higher than those (70–180 K) of  $\text{PbPd}_{1-x}\text{Co}_x\text{O}_2$  and  $\text{PbPd}_{0.9}\text{Mn}_{0.1}\text{O}_2$  reported previously.<sup>2-4</sup> Since  $T_{\text{MI}}$  is the upper temperature limit for good transport properties, our present study may provide a possible way for extending the working temperature range of SGSs to above room temperature.<sup>2</sup> To date, the underlying mechanism for the marked increase in  $T_{\text{MI}}$  remains unclear and, therefore, needs further study. Films with different grain sizes are now under investigation.

Based on the  $\rho$ - $T$  curve, the inset of Fig. 2(a) plots the  $\ln\rho$ - $T^{-1/4}$  and  $\ln\rho$ - $T^{-1}$  curves. Both curves were not linear

<sup>a)</sup>Author to whom correspondence should be addressed. Electronic mail: jcahuang@mail.ncku.edu.tw. Tel.: +886-6-2757575-65266. FAX: +886-6-2747995.

<sup>b)</sup>Electronic mail: cckuo@faculty.nsysu.edu.tw. Tel.: +886-7-5252000-3735. FAX: +886-7-5253709.

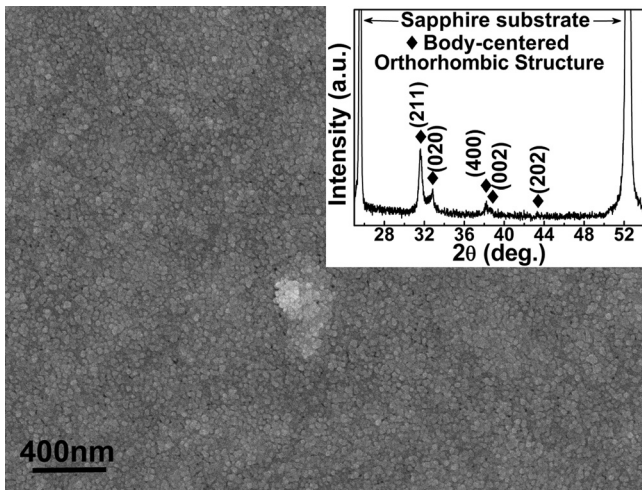


FIG. 1. Surface SEM image of PbPd<sub>0.81</sub>Co<sub>0.19</sub>O<sub>2</sub> film. The inset is the film's XRD pattern.

and the data could not be fitted by the Arrhenius form or the variable range hopping model.<sup>10,11</sup> This indicates that the conduction mechanism for the PbPd<sub>0.81</sub>Co<sub>0.19</sub>O<sub>2</sub> film cannot be attributed to thermally activated behavior due to a band gap or a hopping behavior within localized states. To explain this phenomenon, the relationship between conductivity ( $\sigma$ ) and temperature was fitted using the power law (Fig. 2(b)). The fitting curve coincides with experimental data very well. The power relation between  $\sigma$  and  $T$  indicates that the sample has a gapless band structure.<sup>12,13</sup> The power exponent ( $c$ ) for temperature ranges of 2–100 K and 100–358 K were 0.00322 and 2.23081, respectively. Such a marked difference in power exponent values was likely caused by the competition between two factors—the dopant energy level scattering effect and carrier concentration increasing as temperature

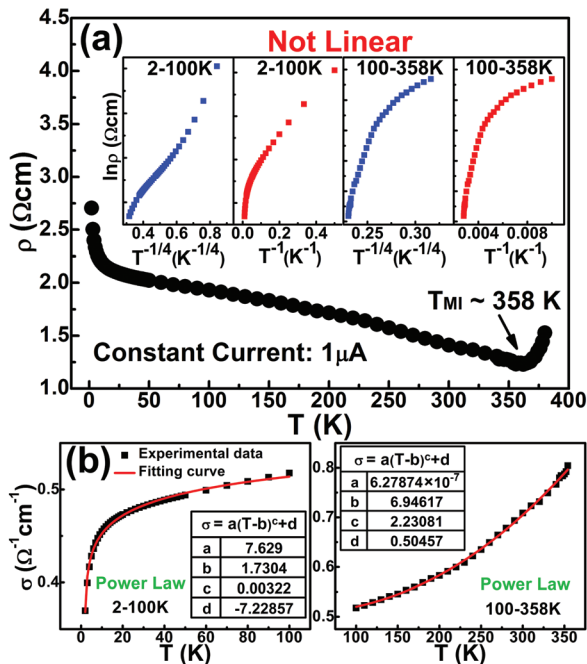


FIG. 2. (Color) (a) Temperature dependence of PbPd<sub>0.81</sub>Co<sub>0.19</sub>O<sub>2</sub> film's resistivity  $\rho$ . The inset shows the relations of  $\ln\rho-T^{-1/4}$  (blue) and  $\ln\rho-T^{-1}$  (red). (b) Experimental data and fitting curves (red line) for the relation between the conductivity  $\sigma$  and the temperature  $T$ .

increased.<sup>13</sup> The influence of the dopant energy level scattering effect is remarkable at low temperatures, while it can be eliminated gradually and the conductivity primarily depends on the intrinsic excitation process at high temperatures.

The film's magnetic properties were measured using a superconducting quantum interference device magnetometer (SQUID) at temperatures of 2–380 K in magnetic fields of –70 to 70 kOe. Figures 3(a) and 3(b) show the  $M$ - $H$  hysteresis loops (the substrate's diamagnetic signal has been subtracted) and the corresponding saturation magnetization  $M_{3T}$  (representing magnetization at 3 T) and coercivity ( $H_c$ ) measured at different temperatures for the same PbPd<sub>0.81</sub>Co<sub>0.19</sub>O<sub>2</sub> film. The film has ferromagnetism at a wide temperature range of 2–380 K (Fig. 3(a)). To determine whether this ferromagnetism is intrinsic or is from impurity phases, this study measured the x-ray absorption near-edge structure (XANES) of the sample on the Co  $K$ -edge at the BL07A beamline of the Taiwan Light Source (TLS), Hsinchu. Figure 4 shows the XANES spectra of the film and the standard Co metal and Co oxides for comparison. Clearly, the XANES spectrum of the sample is entirely different from that of Co metal, meaning that no Co cluster exists in the sample. Therefore, ferromagnetism is not caused by Co cluster. Although the sample's XANES spectrum generally resembles those of Co<sub>2</sub>O<sub>3</sub> and Co<sub>3</sub>O<sub>4</sub>, this study excludes the magnetic origin from these Co oxides because they are not ferromagnetic. That is, ferromagnetism of the sample is intrinsic.

The following two interesting phenomena were also observed (Figs. 3(a) and 3(b)):

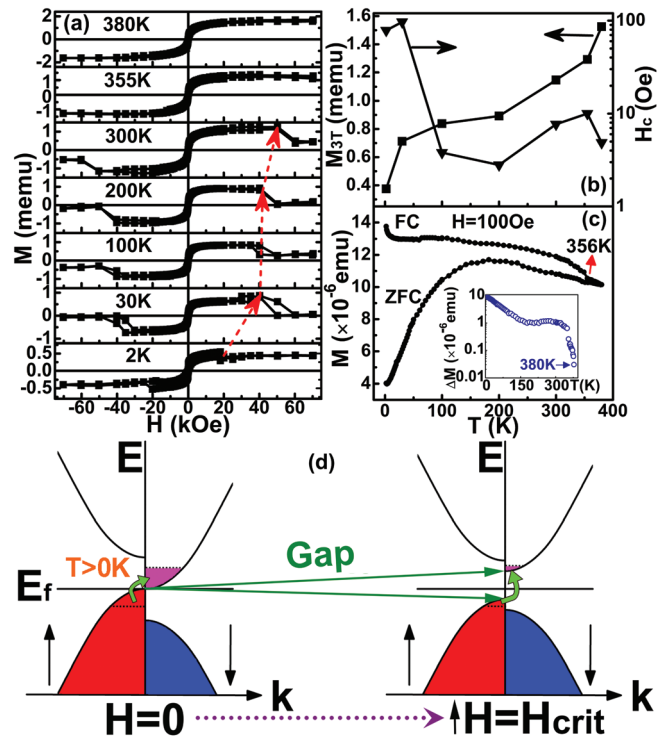


FIG. 3. (Color) (a) Magnetic hysteresis loops of PbPd<sub>0.81</sub>Co<sub>0.19</sub>O<sub>2</sub> film measured at the temperatures of 2, 30, 100, 200, 300, 355, and 380 K. (b) Temperature dependences of film's saturation magnetization  $M_{3T}$  (square) and coercivity  $H_c$  (triangle). (c) FC-ZFC  $M$ - $T$  curve measured at a field of 100 Oe. The inset displays the temperature dependence of the difference  $\Delta M$  between FC and ZFC magnetizations. (d) Schematics of band structure at  $H = 0$  and  $H = H_{crit}$ .

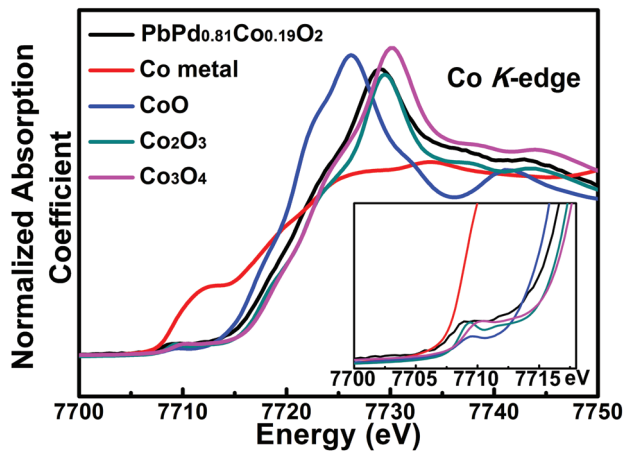


FIG. 4. (Color) Normalized XANES spectrum of  $\text{PbPd}_{0.81}\text{Co}_{0.19}\text{O}_2$  film (black) on Co  $K$ -edge. The spectra of Co (red), CoO (blue),  $\text{Co}_2\text{O}_3$  (olive), and  $\text{Co}_3\text{O}_4$  (purple) are also provided for reference.

- As the temperature increased,  $H_c$  first decreased sharply and then varied within the small range of 2.8–10 Oe, while  $M_{3T}$  increased monotonously. To explain this phenomenon, the field-cooled (FC) and zero-field-cooled (ZFC)  $M$ - $T$  curves (Fig. 3(c)) were measured at a field of 100 Oe. The FC curve diverged from the ZFC curve remarkably at  $<356$  K, while they merged gradually at  $>356$  K. We note that 356 K is near  $T_{\text{MI}}$ , which implies that the magnetic property is correlated with the conduction mechanism. From Fig. 3(c), superparamagnetism and ferromagnetism can also be found coexisting.<sup>14</sup> Because the Co cluster was excluded, superparamagnetism is likely due to the small size of many ferromagnetic nanograins. Superparamagnetism resulted in a marked decrease in  $H_c$  at temperatures  $>100$  K. According to the temperature dependence of the difference  $\Delta M$  between FC and ZFC magnetizations shown in the inset of Fig. 3(c),  $\Delta M$  is nonzero at temperatures  $<380$  K, indicating that the film still has ferromagnetism at high temperatures.<sup>15</sup> The increase in  $M_{3T}$  as temperature increased is the opposite to the normal ferromagnetic material. However, this is a characteristic of the SGS when the special band structure of a  $\text{PbPd}_{1-x}\text{Co}_x\text{O}_2$  SGS, shown in the left schematic of Fig. 3(d), is considered.<sup>1</sup> For such a band structure, more electrons in the valence band can be thermally excited into the conduction band and change its spin direction with the temperature increasing. It is the difference in the number of electrons with opposite spin that results in the increase of the magnetization.
- For films measured at 2–300 K, saturation magnetization ( $M_s$ ) decreased abruptly at some critical field strengths ( $H_{\text{crit}}$ ) by increasing the applied field. Such a  $H_{\text{crit}}$  had a tendency to increase (from roughly 20 to 50 kOe, as indicated by red dashed line in Fig. 3(a)) as measurement temperature increased, while the  $M$ - $H$  loops measured at  $>355$  K had normal ferromagnetic

shapes. For a SGS in a magnetic field, the splitting of Landau levels and the spin splitting of the band can open up a gap between the valence band with majority electrons and the conduction band with minor electrons (Fig. 3(d)) and, thus, causes the decrease in the number of thermally excited conduction electrons, resulting in the decrease in  $M_s$ .<sup>13</sup> If this assumption is correct, the increase in  $H_{\text{crit}}$  can be explained as the result of competition between the number of conduction electrons increasing with temperature and energy gap broadening with the applied magnetic field. Notably, 355 K is also near  $T_{\text{MI}}$ . The magnetic property appears to be strongly correlated with the conduction mechanism again. The underlying physics needs further investigation.

In conclusion, this study prepared a single-phase nanograin-structured  $\text{PbPd}_{0.81}\text{Co}_{0.19}\text{O}_2$  film using the sol-gel spin-coating technique and an oxidation treatment. The film has a gapless band structure feature based on the power dependences of conductivity on temperature. The  $T_{\text{MI}}$  was as high as 358 K. For such a film, the intrinsic ferromagnetism persisted up to 380 K. Due to the existence of many small nanograins, superparamagnetism also existed and, thus, resulted in a marked decrease in  $H_c$  at temperatures  $>100$  K. Additionally, unusual variations in  $M_s$  with the magnetic field and temperature were also observed. The special SGS band structure was likely responsible for these interesting phenomena.

The authors would like to acknowledge the financial support of National Science Council of Taiwan (Nos. NSC 98-2120-M-006-004 and NSC 98-2119-M-006-006). H.L.S and R.Z.Z. acknowledge the partial financial support of the NSFC-50972035 and the NCET-08-0766.

<sup>1</sup>X. L. Wang, *Phys. Rev. Lett.* **100**, 156404 (2008).

<sup>2</sup>X. L. Wang, G. Peleckis, C. Zhang, H. Kimura, and S. Dou, *Adv. Mater.* **21**, 2196 (2009).

<sup>3</sup>K. J. Lee, S. M. Choo, J. B. Yoon, K. M. Song, Y. Saiga, C. Y. You, N. Hur, S. I. Lee, T. Takabatake, and M. H. Jung, *J. Appl. Phys.* **107**, 09C306 (2010).

<sup>4</sup>K. J. Lee, S. M. Choo, Y. Saiga, T. Takabatake, and M. H. Jung, *J. Appl. Phys.* **109**, 07C316 (2011).

<sup>5</sup>L. M. Sandratskii and P. Bruno, *J. Phys.: Condens. Matter* **15**, L585 (2003).

<sup>6</sup>Y. F. Li, Z. Zhou, P. W. Shen, and Z. F. Chen, *ACS Nano* **3**, 1952 (2009).

<sup>7</sup>Y. F. Pan and Z. Q. Yang, *Phys. Rev. B* **82**, 195308 (2010).

<sup>8</sup>X. L. Wang, S. Dou, and C. Zhang, *NPG Asia Mater.* **2**, 31 (2010).

<sup>9</sup>H. L. Su, N. J. Tang, B. Nie, S. L. Tang, R. L. Wang, M. Lu, S. Y. Zhang, L. Y. Lv, and Y. W. Du, *Thin Solid Films* **515**, 7066 (2007).

<sup>10</sup>G. Hu and H. Gong, *Acta Mater.* **56**, 5066 (2008).

<sup>11</sup>A. J. Behan, A. Mokhtari, H. J. Blythe, D. Score, X. H. Xu, J. R. Neal, A. M. Fox, and G. A. Gehring, *Phys. Rev. Lett.* **100**, 047206 (2008).

<sup>12</sup>A. A. Vaipolon, S. A. Kijaev, L. V. Kradinova, A. M. Polubotko, V. V. Popov, V. D. Prochukhan, Y. V. Rud, and V. E. Skoriukin, *J. Phys.: Condens. Matter* **4**, 8035 (1992).

<sup>13</sup>I. M. Tsidilkovski, G. I. Harus, and N. G. Shelushinina, *Adv. Phys.* **34**, 43 (1985).

<sup>14</sup>N. Akdogan, H. Zabel, A. Nefedov, K. Westerholt, H. W. Becker, S. Gök, R. Khaibullin, and L. Tagirov, *J. Appl. Phys.* **105**, 043907 (2009).

<sup>15</sup>D. S. Han, S. Y. Bae, H. W. Seo, Y. J. Kang, J. Park, G. Lee, J. P. Ahn, S. Kim, and J. Chang, *J. Phys. Chem. B* **109**, 9311 (2005).